



Cite this: *Environ. Sci.: Adv.*, 2024, **3**, 912

A comparison of carbon dot and CdTe quantum dot toxicity in *Drosophila melanogaster*[†]

Shawninder Chahal,^a Jun-Ray Macairan,^a Hoai-Nam N. Bui,^b Anthony Smith,^b Hans C. E. Larsson,^b Rafik Naccache  ^c and Nathalie Tufenkji  ^{*a}

Carbon dots (CDs) are carbon nanoparticles that are typically \sim 10 nm in size and feature many properties similar to quantum dots (QDs). Cadmium telluride QDs (CdTeQDs) are a frequently studied QD since their size, and therefore fluorescence spectra, can be easily controlled. However, cadmium is known to be toxic, making its use in consumer goods limited or outright banned in many jurisdictions. While many studies have examined the toxicity of CDs and CdTeQDs, few have directly compared both nanoparticles under the same conditions. Herein, we provide a direct comparison of the toxicity of nitrogen-doped CDs (NCDs), nitrogen, sulfur co-doped CDs (SCDs), and CdTeQDs in the model organism *Drosophila melanogaster* (fruit fly). No impact on the development of larvae into adult flies from NCDs or SCDs in the 10–100 mg kg^{−1} food range was observed, whereas an EC₅₀ of 46 mg kg^{−1} CdTeQDs in food was observed. A strong positive correlation was found between the concentration of CdTeQDs in food and the mean pupation and eclosion time, indicating severe developmental delays as CdTeQD concentration increased. Further experiments at sublethal concentrations revealed no significant difference between any of the treatments when evaluating reproductive performance, larval crawling, and fly climbing ability. Gut tube anatomy did differ between control and treatment flies, with all treatment individuals expressing lengthened, and in some cases, distended midguts. This work demonstrates that both NCDs and SCDs are considerably less toxic than CdTeQDs in the 10–100 mg kg^{−1} food range, further enabling the former's potential applications for biocompatible QD-like nanomaterials.

Received 24th January 2024
Accepted 19th April 2024

DOI: 10.1039/d4va00017j
rsc.li/esadvances

Environmental significance

CdTe quantum dots (QDs) are nanoparticles with remarkable properties, but their high toxicity limits their use in consumer goods and biomedical applications. Therefore, a less toxic and more sustainable alternative that exhibits similar properties to QDs would be desirable. Carbon dots (CDs), seek to fill that gap, by displaying many similar properties to QDs, while being less toxic, and in some cases, being synthesized from naturally occurring compounds. This work directly compares the toxicity of nitrogen-doped CDs, nitrogen, sulfur co-doped CDs, and CdTeQDs, to *Drosophila melanogaster*, revealing that these CDs are considerably less toxic than the CdTeQDs, granting insight into their potential as a sustainable alternative to CdTeQDs.

1 Introduction

Quantum dots (QDs) are semiconductor nanoparticles that exhibit unique properties when compared to their bulk counterparts. Notably, QDs exhibit quantum confinement effects, a phenomenon that links a QD's bandgap and fluorescence (within the UV, visible, and near-infrared range) to its size.¹ This property, along with their reduced photobleaching compared to

organic dyes,¹ has enabled the use of QDs in a variety of applications such as: bioimaging,² solar cells,³ light-emitting diodes,⁴ and chemical sensing⁵ to name a few.

Original QDs included CdS, CdSe, and CdTe nanocrystallites that were synthesized through the injection of organometals in a high-temperature solvent.⁶ However, cadmium is an element with known toxicity often translating into cadmium-derived QD toxicity. For instance, Liu *et al.* found that CdSeQDs can accumulate in the liver of mice, inducing morphological changes to their hepatic lobules and increased oxidative stress.⁷ Particularly concerning is the fact that these QDs were found to be more toxic than cadmium ions, suggesting that QD toxicity is not caused by cadmium alone.⁷ Even after coating CdSe with a less toxic compound such as ZnS, the resulting CdSe/ZnS-QDs can still nick DNA due to free radical generation.⁸ CdTeQDs have also shown similar toxic effects in mouse liver and AML12 cells causing increased oxidative stress and apoptosis.⁹

^aDepartment of Chemical Engineering, McGill University, Montreal, Quebec H3A 0C5, Canada. E-mail: nathalie.tufenkji@mcgill.ca; Fax: +514-398-6678; Tel: +514-398-2999

^bRedpath Museum, McGill University, Montreal, Quebec H3A 0C4, Canada

^cDepartment of Chemistry and Biochemistry and the Centre for NanoScience Research, Concordia University, Montreal, Quebec H4B 1R6, Canada

† Electronic supplementary information (ESI) available. See DOI: <https://doi.org/10.1039/d4va00017j>



CdTeQDs are likewise known to be toxic towards zebrafish,¹⁰ *Hydra vulgaris*,¹¹ and *Bombyx mori*.¹²

Carbon dots (CDs) are a type of carbon nanoparticle that exhibits properties similar to quantum dots. For instance, both nanoparticles are typically less than 10 nm in size and have excitation and emission wavelengths in the UV-visible range which enable them to be used in similar applications.¹³ Carbon dots have therefore garnered attention as a potentially safer alternative to metallic QDs. They are also being increasingly synthesized from renewable raw materials and compounds, further increasing the sustainability of CD use over QDs.¹³ A fascinating example of both the safer and more renewable nature of carbon dots was observed in a study by Qu *et al.* in which they synthesized CDs from citric acid and urea.¹⁴ They subsequently used their CDs to create fluorescent ink and demonstrated its safety by applying it to human skin.¹⁴ In addition, there exists an emerging literature of CD studies exploring applications in bioimaging and chemical sensing whereby their less toxic nature can give them an advantage over cadmium-derived QDs.¹³

Various organisms have been utilized for studying nanoparticle toxicity. Among them, *Drosophila melanogaster*, more commonly known as the fruit fly, has proven to be an interesting model organism for the study of nanoparticle toxicity.¹⁵ For instance, it has been found that 77% of human disease genes have a highly similar related gene in flies.¹⁶ Moreover, a single mating pair can produce hundreds of offspring in under two weeks whereas mammalian models produce considerably fewer offspring on the order of months.¹⁷ Flies also have several structures that play a similar role to the mammalian heart, lung, kidney, gut, and reproductive tract.¹⁷ In addition, the effect of several central nervous system drugs on flies has been shown to be similar to their effect on mammals.¹⁷ Common routes by which nanoparticles may result in toxicity include ingestion, inhalation, and surface contact, leading to oxidative stress, which can in turn impact the lifespan and fecundity of the flies and result in genotoxicity and metabolic defects.¹⁵ Specifically, CdSeQDs are known to be toxic to flies by penetrating the intestine of larvae and eventually interacting with hemocytes, causing genotoxicity and elevated reactive oxygen species production.¹⁸ The release of Cd²⁺ from the QDs is thought to play a major role in the observed toxicity.¹⁸

Few studies directly compare CD toxicity with that of Cd-derived QDs. For instance, Xiao *et al.* evaluated the toxicity of CDs and CdTeQDs in the microalgae *Chlorella pyrenoidosa* finding that the CdTeQDs had an EC₅₀ of 0.015 mg L⁻¹ which was orders of magnitude lower than the EC₅₀ of 38.56–232.47 mg L⁻¹ they measured for the three types of CDs they tested.¹⁹ Herein, we evaluate and compare the toxicity of CDs and CdTeQDs in a model animal organism, *Drosophila melanogaster*. It has been well established in the literature that doping CDs with heteroatoms, such as nitrogen and sulfur, typically increases the quantum yield of the CD.²⁰ Therefore, we assessed the toxicity of two commonly doped types of CDs, nitrogen-doped CDs (NCDs) and sulfur, nitrogen co-doped CDs (SCDs), to determine if their toxicity profile would differ because of their unique chemical functional groups.

2 Experimental

2.1 Synthesis of NCDs

Synthesis of NCDs was done according to previously reported methods, with some modification.²¹ Briefly, 7.2 g of L-phenylalanine (Sigma-Aldrich, P2126) and 2.1 g of citric acid (Sigma-Aldrich, 251275) were added to 20 mL of MilliQ water in a glass microwave reaction vial. The reaction mixture was placed into the microwave reactor (CEM Discover SP) and initially heated at 100 °C for 5 min with stirring to completely dissolve the reagents in water. Afterwards, the reaction mixture was allowed to heat to a temperature of 200 °C for 12 min with stirring. The resulting suspension was left to cool naturally to room temperature. The purification process is described in Section 2.3.

2.2 Synthesis of SCDs

Synthesis of SCDs was done according to previously reported methods, with some modification.²² Briefly, 0.689 g of L-glutathione (Sigma-Aldrich, G4251) was mixed into 20 mL of formamide (Sigma-Aldrich, F7503). The mixture was sonicated for 15 min until it became clear. The reaction medium was then poured into a glass microwave reactor vial and heated to 180 °C for 5 min with stirring. The resulting suspension was left to cool naturally to room temperature. The purification process is described in Section 2.3.

2.3 Purification of carbon and quantum dots

Purification of CDs and QDs was done according to previous methods with some modifications.²² The CdTeQDs (Plasma-Chem, PL-QDN-610) were suspended in water (concentration: 1.4 mg mL⁻¹). The CD suspension (post-synthesis mixture) or QD suspension was filtered using a 0.2 µm nylon filter (Millipore, SLGN033) to remove any large particles. The CD or QD dispersions were dialyzed using a cellulose ester dialysis membrane with a molecular weight cut-off of 3.5–5.0 kDa (Repligen, 132725) to remove unreacted materials and intermediates from the CD suspensions, and to ensure similar sample preparation in the QD suspensions. The samples were dialyzed in 1 L of type 1 water over 5 days with the water changed twice a day. The nanoparticles were then filtered using a 0.2 µm nylon filter to remove any aggregates. For the control treatment, water alone was processed in the same manner and was later added to the fly food, to ensure that all treatments were treated as similarly as possible. At this point, the CdTeQDs remained in suspension and were diluted as needed for further use.

To remove any remaining impurities, the SCD suspensions were washed twice with ethanol and then twice with acetone (*i.e.*, until the supernatant was colourless). On the other hand, due to their enhanced dispersibility in ethanol, the NCD suspensions were washed four times with acetone. The first wash consisted of a 1 : 10 (suspension : solvent) volume ratio. After centrifugation at 10 000g for 10 min, the precipitate was resuspended in fresh solvent for the next wash step. The precipitate was then dried overnight at 70 °C. The dried



nanomaterials were then resuspended in water at the desired concentration.

2.4 Characterization of carbon dots and quantum dots

X-ray photoelectron spectroscopy (XPS) measurements were taken using a Thermo Fisher Scientific K-Alpha X-ray Photoelectron Spectrometer System. Fourier-transform infrared (FTIR) spectroscopy was performed using a Nicolet iS5 FTIR spectrometer. Transmission electron microscopy (TEM) images were obtained using a Thermo Scientific Talos F200X G2 (Facility for Electron Microscopy Research, McGill University) for the QDs and an LVEM5 benchtop electron microscope for the CDs. Quantum yields were measured using an FLS920 fluorescence spectrometer (Edinburgh Instruments). Fluorescence spectroscopy and UV-vis measurements were performed using a Horiba Fluorolog-QM.

2.5 *Drosophila melanogaster* husbandry

Fruit flies were reared according to methods described previously, with some modification.²³ *Drosophila melanogaster* (Oregon-R strain) were reared in a food mixture consisting of: 84.6 wt% reverse osmosis (RO) water (type II, $> 1 \text{ M}\Omega$), 14.9 wt% Nutri-Fly Bloomington Formulation powder (Diamed, GEN66-112), and 0.5 wt% sodium propionate (Genesee Scientific, 20-271) in a *Drosophila* culture bottle (Carolina, 173135). These culture bottles were kept in a Versatile Environmental Test Chamber (Panasonic, MLR-352H-PA) operating under a day/night cycle at 60% relative humidity at 25 °C. Days consisted of illumination at ~ 1500 lx for 12 h. Nights consisted of complete darkness for 12 h.

2.6 Larvae collection

When a larger quantity of flies was needed, embryo collection cages (Diamed, GEN59-101) were set up according to methods described previously, with some modification.²⁴ Briefly, one packet of FlyStuff grape agar premix (Diamed, GEN47-102) was mixed into 500 mL of RO water and autoclaved. The contents were then poured into multiple 100 mm Petri dishes (Fisher Scientific, FB0875713). Next, 15 g of inactive dry yeast nutritional flake (Diamed, GEN62-106) was mixed with 15 mL of RO water to create a yeast paste which was then spread onto the center of the grape agar plate. Flies were transferred to the embryo collection cage, which was placed on top of the grape agar plate where the flies then laid eggs. This moment is referred to as day 0. The grape agar plate containing eggs was removed from the cage after 4 h. Approximately 24 h later, the eggs that had transformed into larvae were then used for subsequent experiments as described in the following sections unless stated otherwise.

2.7 Carbon dioxide anesthesia

When a specific selection of flies was required (e.g., obtaining an equal amount of female and male flies), flies were anesthetized with CO₂ on a Flystuff Flypad (Genesee Scientific, 59-114) and sorted as needed. Total anesthesia time was restricted

to less than 10 min to minimize undesirable physiological effects on the flies.²⁵

2.8 Developmental toxicity

Developmental toxicity was measured according to previous methods with some modifications.²⁴ Briefly, NCDs, SCDs, or CdTeQDs were mixed into fly food such that the final concentration in food was 0, 10, 40, 70, or 100 mg kg⁻¹. Thereafter, 10 mL of the treated or control (CTRL) fly food was added into a 50 mL glass test tube and capped with a cotton plug. Approximately twenty larvae were then transferred from grape agar plates into the test tube. The number of pupae and adult flies were counted every 2 days until day 14. We note that during the counting process, if any flies were present in the test tube, they were removed from the test tube for counting and not returned. This allowed for accurate counting of the flies over time by ensuring that any flies counted must have emerged during the previous 48 h. Each treatment or control was replicated with 1–3 test tubes simultaneously. The entire experiment was performed in three experimental blocks for a final count of $N = 6$. For example, if block 1 had $N = 2$ and block 2 had $N = 1$, then block 3 would have $N = 3$. This was due to fluctuations in the number of eggs obtained in each batch since we cannot guarantee that the exact same number of flies would be present during each egg collection cycle, and we avoid cross-contamination by only using one Petri dish of eggs per nanoparticle type.

2.9 Sublethal toxicity assays

The results from the developmental toxicity study allowed us to determine a sublethal concentration of NCDs, SCDs, and CdTeQDs in food at which to measure other endpoints. The use of a sublethal dose minimizes survivorship bias, allowing for a more reliable measure of the sublethal toxic effects of NCDs, SCDs, and CdTeQDs. Briefly, NCDs, SCDs, or CdTeQDs were mixed into fly food such that the final concentration was either 100 mg kg⁻¹ NCD, 100 mg kg⁻¹ SCD, or 5 mg kg⁻¹ CdTeQD. A control was also made. Thereafter, 10 mL of the treated or control fly food was added into a 50 mL glass test tube and capped with a cotton plug. Each assay began with approximately 20 first instar larvae being transferred from a grape agar plate into the test tube. The test tube was closed with a cotton plug.

2.9.1 Reproductive performance assay. The reproductive performance of flies was measured according to previous methods with some modification.²⁶ On day 9, any adult flies present in the treated or control test tubes were removed. Approximately 4 h later, newly emerged flies were placed under CO₂ anesthesia. One female and one male fly were transferred into a new test tube with control fly food (i.e., that does not contain NCDs, SCDs, or CdTeQDs). The mating pair was transferred to a new test tube every two days for 10 days. The number of pupae and adult flies that emerged from each test tube that the mating pair laid eggs in was recorded 14 days after the parents first entered the test tube. Each treatment or control was replicated with 3–6 test tubes simultaneously. The entire



experiment was performed in two experimental blocks for a final replicate count of $8 \leq N \leq 12$.

2.9.2 Larval crawling assay. The peristalsis of larvae was measured as done previously with some modifications.²⁴ On day 4, three larvae were removed from the treated or control test tube and, one at a time, placed on a 100 mm Petri dish containing grape agar. The larva was allowed 30 s to adjust to their new environment and the Petri dish was then video recorded under an Olympus SZX16 stereo microscope for 60 s. The larva was then removed from the dish and the next larva was placed on the grape agar plate and the cycle started again. Each treatment group had its own dish, to avoid cross-contamination from larvae exposed to different nanoparticles. The average number of peristaltic contractions per min of the three larvae from a single test tube was taken and represented a single data point. Each treatment or control was replicated with three test tubes in parallel. The entire experiment was performed in two experimental blocks for a final replicate count of $N = 6$.

2.9.3 Climbing and fly mass assay. A climbing assay was performed according to methods described previously, with some modification.²⁷ On day 11, the flies were transferred from the treated or control test tube to a 100 mL graduated cylinder marked at a height of 10 cm that was then capped with a cotton plug. The cylinder was tapped to move the flies to the bottom. The flies were then left to ascend while being video recorded. After 10 s, the number of flies that crossed the 10 cm mark was divided by the total number of flies in the graduated cylinder. This process was performed five times. The average of these five trials was taken and represented a single replicate of data.

The flies from the climbing assay were then placed under CO₂ anesthesia and separated into male and female groups. The collective mass of each sex of flies was measured and divided by their respective number of flies and represented a single replicate of data.

Each treatment or control was replicated with 2–3 test tubes simultaneously. The entire experiment was performed in two experimental blocks for a final replicate count of $5 \leq N \leq 6$.

2.9.4 Locomotor activity monitoring. Locomotor activity monitoring was done according to previously reported methods with some modifications.²⁸ On day 11, one male fly (from a treated or control test tube) was placed in a glass tube ($L \times D$: 65 mm \times 5 mm) with control fly food (*i.e.*, that does not contain NCDs, SCDs, or CdTeQDs) at one end and a cotton plug at the other end. A *Drosophila* Activity Monitor (DAM2, TriKinetics) was used with 32 tubes fitted in it (8 control, 8 NCD, 8 SCD, and 8 CdTeQD). The activity monitor counted the number of times per minute that the fly would interrupt a beam of infrared light at the middle of the tube. The flies were given 24–48 h to adjust to their new environment and then flies went through 3 days of a light-dark cycle consisting of 12 h light, 12 h dark. The experiment started at the beginning of the first 12 h light phase. If any tube showed zero counts in the final 24 h, then the fly was presumed dead, and removed from the analysis. Two DAM2 units ran in parallel (*i.e.*, 16 tubes per treatment or control simultaneously). The entire experiment was performed in two experimental blocks for a final replicate count of $31 \leq N \leq 32$ after the removal of dead flies.

2.10 Light sheet fluorescence microscopy

Light sheet fluorescence microscopy (LSFM) was performed, according to previously reported methods with some modification.²⁹ On day 11, female flies were taken to determine if there was any uptake of the NCDs, SCDs, or CdTeQDs. Flies were stored in refrigerated (4 °C) 10% neutral-buffered formalin for 24–48 h. To increase the depth penetration of light and reduce light scattering, the fly samples were placed in a tissue clearing solution (550 g L⁻¹ of urea, 225 g L⁻¹ of sorbitol), and 50 g L⁻¹ of Triton X-100).

Flies were mounted in a 1 mL syringe containing ScaleS4 mounting solution (15 g L⁻¹ of agarose, 240 g L⁻¹ of urea, 400 g L⁻¹ of sorbitol, 100 g L⁻¹ of sorbitol, and 150 g L⁻¹ of dimethyl sulfoxide in water) with 2.0% low melting point agarose as developed by Hama *et al.*³⁰ The refractive index of the mounting media was adjusted with glycerol or water until it reached a value of 1.44. The chamber of the Zeiss light sheet Z.1 microscope was filled with ScaleS4 to ensure a consistent index of refraction with the sample. A 5 \times 0.1 NA objective was used for illumination and a 5 \times 0.16 NA objective was used for detection.

2.11 Nano-computed tomography

Nano-computed tomography (Nano-CT) was performed, as reported previously with some modification.²⁴ On day 11, female flies were taken to determine if there was any damage to the fly gut. The flies were placed in a fixative (FAE) consisting of 59 vol% ethanol, 35 vol% formalin (40% formaldehyde in water), and 6 vol% glacial acetic acid. After 24 h, the flies were transferred to 70 vol% ethanol and stored in the fridge to be used later. When the flies were ready to be imaged, they were placed in 50 vol% ethanol for 20 minutes, then 25 vol% ethanol for another 20 minutes. The flies were then decapitated with a scalpel and placed in 10 g L⁻¹ phosphotungstic acid hydrate. The phosphotungstic acid was refreshed 9 times over the span of 29 days. The flies were then transferred to 25 vol% ethanol for 20 minutes, then 50 vol% ethanol for 20 minutes, and then 70 vol% ethanol for 20 minutes. Three flies were then submerged in 70 vol% ethanol in a 200 μ L pipette tip, another pipette tip was placed on top to secure the flies in place, and the top and bottom were wrapped in parafilm.

Images were acquired on a Zeiss Xradia 520 between 1–3 μ m resolution with a 4 \times objective lens with 2 \times 2 camera binning over a 360 degree-rotation. A total of 2401 and 401 projections were taken in high- and low-resolution scans, respectively, at 60 kVp and 82 μ A. All high-resolution scans were taken using an LE1 filter and 0.5 s exposure. In low resolution scans, the same filters were used with 1–2.5 s exposure. The resulting images were qualitatively analyzed, and 3D gut tube models were reconstructed with Dragonfly software, Version 2020.2 (Object Research Systems Inc.).³¹ Figures were produced using Blender software, Version 2.80.75.³² Although three flies were present for each treatment during imaging, not all flies produced useable images. Therefore, we had 3 useable CTRL images and 2 useable images for each of the NCD, SCD, and CdTeQD treatments.



2.12 Statistical analysis

Data was first tested for normality of the residuals using the Shapiro-Wilk test. The data was then tested for equal variance among groups using Bartlett's test. If both these tests validated the assumption of normality and equal variance, then statistical significance was measured using an *n*-way analysis of variance (*n*-way ANOVA). If the ANOVA showed a significant difference among treatments, then a Tukey-Kramer test was performed for sublethal toxicity assays. However, if the data did not pass the test of normality or equal variance, then *n* Kruskal-Wallis *H* tests were performed, followed by a Mann-Whitney *U* test with Bonferroni correction where significant differences were observed for sublethal toxicity assays. For the developmental toxicity assay, when significant differences were observed between concentrations for a given treatment and the number of pupae or flies was monotonically decreasing with concentration, then a Hill equation (eqn (1)) was fit to the data to obtain a half maximal effective concentration (EC_{50}) value. When significant differences in emergence time were observed between concentrations for a given treatment, a linear regression was performed. Throughout all statistical tests, $p < 0.05$ was considered as significant. Data analysis and visualization was performed in Python 3.9.12 using numpy 1.21.5,³³ pandas 1.4.2,^{34,35} scipy 1.7.3,³⁶ statsmodels 0.13.2,³⁷ and matplotlib 3.5.1.³⁸

The Hill equation takes the form of:

$$\frac{x - \mu_{CTRL}}{\mu_{MAX} - \mu_{CTRL}} = \frac{1}{1 + \left(\frac{EC_{50}}{[NP]} \right)^n} \quad (1)$$

where x is the number of pupae or flies after 14 days; μ_{CTRL} is the mean number of pupae or flies after 14 days in the control; μ_{MAX} is the maximum response (*i.e.*, 0 pupae or flies), EC_{50} is the half maximal effective concentration, $[NP]$ is the concentration of NCDs, SCDs, or CdTeQDs in food; and n is the Hill coefficient.

3 Results and discussion

3.1 Characterization of carbon and quantum dots

Quasi-spherical dots were obtained following their synthesis as shown *via* TEM (Fig. S1†). The size of the NCDs and SCDs were measured using TEM, with mean diameters of 7.4 nm (Fig. S1a†) and 7.0 nm (Fig. S1b†), respectively. The CdTeQDs were ~3.5 nm according to the manufacturer's specifications. TEM of the CdTeQDs (Fig. S2†) revealed their spherical shape with a median diameter of 3.6 nm and a mean diameter of 4.8 nm. We hypothesize that the higher mean size may be due to aggregated particles since the median size is similar to the manufacturer's specifications.

The FTIR spectra for the NCDs, SCDs, and CdTeQDs are shown in Fig. S3.† From the spectrum of the NCDs, the peak at 1703 cm⁻¹ is indicative of C=O stretching stemming from the presence of carboxylic acids and aliphatic ketones, while the presence of C-N is confirmed with the band at 1389 cm⁻¹. The SCDs showed a broad peak centered at 3330 cm⁻¹ stemming

from the symmetric and asymmetric stretching of N-H and O-H groups, while stretching of C=O (from amide), C-OH, and C-N groups were observed at 1665, 1596, and 1384 cm⁻¹, respectively. The CdTeQDs showed a broad peak centered around 3400 cm⁻¹ originating from O-H stretching. The peak at 1543 cm⁻¹ corresponds to C=O stretching, whereas the band at 1405 cm⁻¹ corresponds to the C-O-H in-plane bending. Nitrogen doping of the NCDs was confirmed using XPS where the atomic percent composition was determined to be 52% C, 38% O, 10% N (Fig. S4†). Similarly, both nitrogen and sulfur doping of the SCDs were confirmed using XPS with an atomic percent composition of 51% C, 27% O, 19% N, 2.9% S (Fig. S5†).

The quantum yield of the CdTeQDs, NCDs, and SCDs were 21.9%, 17.2%, and 7.3%, respectively. The fluorescence spectra of the CdTeQDs, NCDs, and SCDs are shown in Fig. S6† with emission peaks at 615 nm, 482 nm, and 681 nm, respectively. For both quantum yield and fluorescence measurements, an excitation wavelength of 561 nm was used for CdTeQDs and 405 nm for NCDs and SCDs to match their respective excitation wavelengths used in LSFM. The UV-vis spectra of the CdTeQDs, NCDs, and SCDs are shown in Fig. S7.† NCDs possess an absorption band at 340 nm that is attributed to the $n \rightarrow \pi^*$ transition of C=O bonds;³⁹ in contrast, SCDs showed several prominent bands at 418 nm and 580–700 nm, which are attributed to $\pi \rightarrow \pi^*$ and $n \rightarrow \pi^*$ transitions of the aromatic sp² network for C=O and C=S/C=N bonds, respectively.⁴⁰ While the UV-vis spectrum of CdTeQDs was mostly monotonically decreasing, it briefly inverted at 558–560 nm before continuing to decrease. This range was close to the LSFM excitation wavelength used (*i.e.*, 561 nm).

3.2 Developmental toxicity

The toxicity of the SCDs in HeLa cells was previously shown to have a half maximal inhibitory concentration (IC_{50}) of 148 mg L⁻¹.²² We note, however, that mechanisms involved in *in vitro* toxicity may differ considerably *in vivo*, and the original work demonstrated that 100 mg L⁻¹ was a sufficient and safe concentration for bioimaging purposes.²² Moreover, our preliminary screening of CdTeQDs indicated that a half maximal effective concentration (EC_{50}) was likely to be found somewhere near the center of the 10–100 mg kg⁻¹ CdTeQD range. As a result, we wanted to examine a CD concentration range that may be used in practice, and that also matches the relevant range over which CdTeQD toxicity manifests. Therefore, the developmental toxicity of the NCDs, SCDs, and CdTeQDs on 1st instar larvae's development into pupae and adult flies was measured over the concentration range of 10–100 mg kg⁻¹ food. No significant dose-response was observed in the total number of pupae and flies emerging from the larvae exposed to NCDs or SCDs (Fig. 1a and b). We note that significant differences were observed between experimental blocks in the NCD treatments. While several studies have examined the toxicity of CDs, few have compared them directly to quantum dots that may be used in similar applications. We found that there was a significant dose-response observed in the total number of pupae ($p = 2.3 \times 10^{-4}$) and flies ($p = 7.6 \times 10^{-5}$)



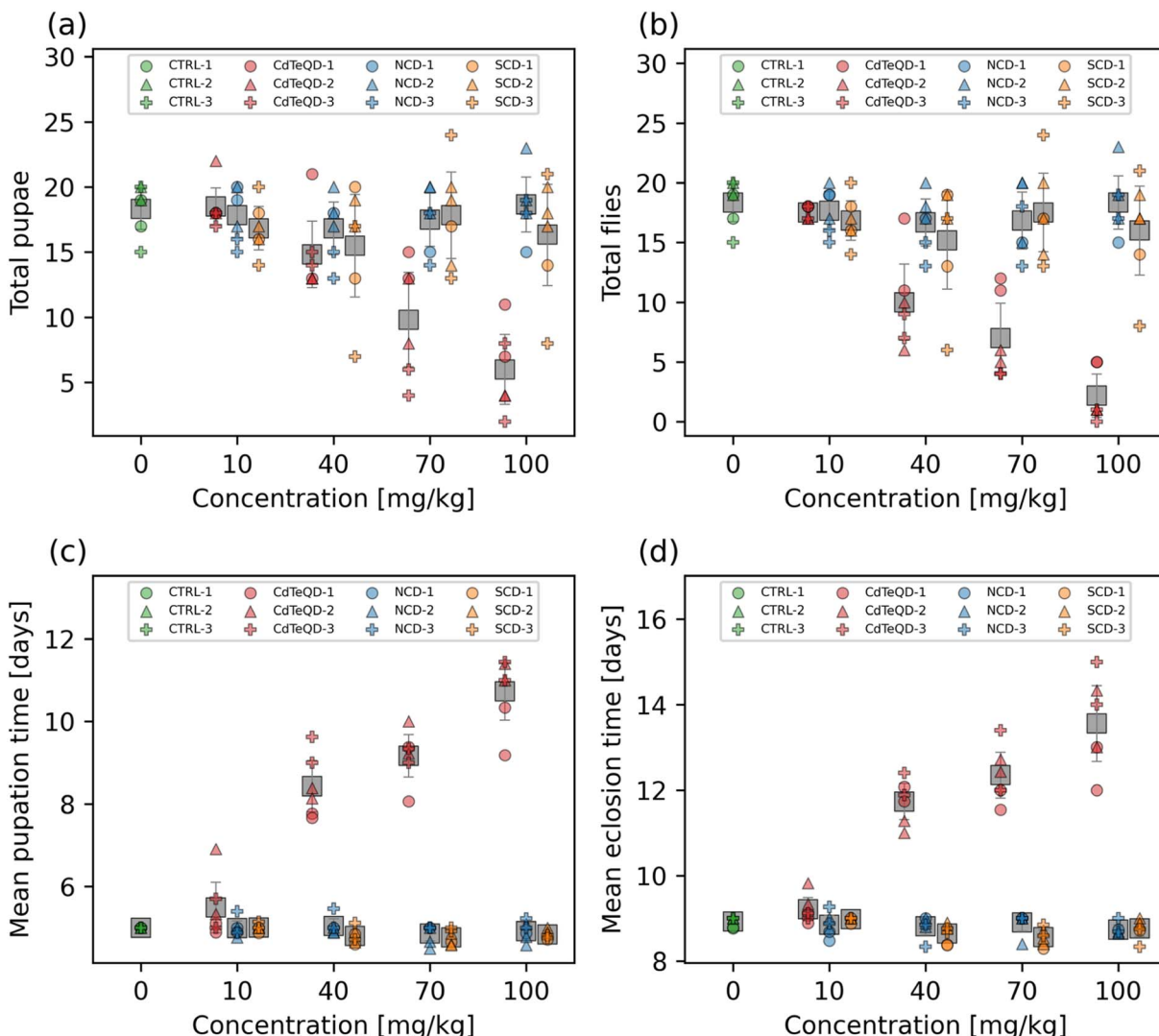


Fig. 1 Number of (a) pupae and (b) flies that emerged from approximately twenty first instar larvae raised on 0, 10, 40, 70, or 100 mg kg^{-1} NCD, SCD, or CdTeQD treated food by day 14. The mean (c) pupation and (d) eclosion time of the pupae and flies in (a) and (b), respectively. Grey squares represent the mean of data points in that column and error bars represent $2 \times$ the standard error of the mean. Legend labels have the format X-Y where X is the treatment and Y is the experimental block ID.

emerging from the larvae exposed to CdTeQDs (Fig. 1a and b). No significant differences were observed between experimental blocks for both pupae and flies. Fitting data to the Hill equation revealed that the EC_{50} of the CdTeQDs on larval development into pupae was $74 \pm 6.0 \text{ mg kg}^{-1}$ food, and into flies was $46 \pm 4.7 \text{ mg kg}^{-1}$ food (mean \pm standard error). These curve fits are shown in Fig. S8.† This discrepancy between the EC_{50} values in pupae and flies becomes clearer when examining the eclosion fraction, *i.e.*, the fraction of pupae that successfully eclose into flies. No significant dose-response was observed in the eclosion fraction of pupae exposed to NCDs or SCDs (Fig. S9†). Conversely, significant differences in the eclosion fraction of pupae were found between CdTeQD treatment concentrations ($p = 2.5 \times 10^{-4}$) (Fig. S9†). However, since the data did not fit the shape of the Hill equation, no curve fitting was performed on the eclosion fraction data. Moreover, we note that there were

no significant differences between experimental blocks for any of the treatments when measuring the eclosion fraction.

Another important metric in evaluating developmental toxicity is the time it takes for larvae to develop into pupae and adult flies. Delays in development time can be lost when screening just for mortality. No dose-response was observed in the mean pupation or eclosion time of larvae exposed to NCDs (Fig. 1c and d). We remark that significant differences were observed between experimental blocks ($p = 0.037$) in the mean pupation time of NCD-exposed larvae. While a significant dose-response was observed from the SCDs on the mean pupation ($p = 0.012$) and eclosion ($p = 2.1 \times 10^{-3}$) time (Fig. 1c and d), a linear regression revealed that both showed a weak negative correlation (pupation: $r = -0.49$, eclosion: $r = -0.46$) (Fig. S10†). The CdTeQDs also showed a significant dose-response on the mean pupation ($p = 4.6 \times 10^{-5}$) and eclosion

time ($p = 5.5 \times 10^{-5}$) (Fig. 1c and d). In this case, a linear regression revealed a strong positive correlation for both mean pupation ($r = 0.94$) and eclosion ($r = 0.93$) time (Fig. S10†). The slopes of the regressions indicated that increasing the CdTeQD concentration in the food by 1 mg kg^{-1} would delay pupation by 83 min and eclosion by 68 min at concentrations below 100 mg kg^{-1} . No significant differences were observed between experimental blocks in the mean pupation or eclosion time of larvae exposed to SCDs or CdTeQDs.

Interestingly, Chousidis *et al.* also investigated the toxicity of undoped, N-doped, and N,S co-doped CDs in zebrafish, finding that they had an LD_{50} of 584 mg L^{-1} , 400 mg L^{-1} , and 150 mg L^{-1} , respectively.⁴¹ These results are all well above the highest concentration we examined (100 mg kg^{-1}), however, Chousidis *et al.* did report an LD_{25} of 63 mg L^{-1} for their N,S co-doped CDs,⁴¹ whereas our SCDs did not show any developmental toxicity near this concentration. This further emphasizes the importance of conducting toxicity studies in a multitude of environments and organisms, especially when comparing results from aquatic and terrestrial organisms. While both organisms must consume nanoparticles through their diet, the aquatic organism must also be submerged in it for the entirety of the exposure, allowing for the nanoparticle to enter the organism *via* more routes of exposure. Moreover, Chousidis *et al.* synthesized their N,S co-doped CDs from citric acid and thiourea,⁴¹ whereas we synthesized ours from glutathione and formamide, therefore it is likely that there are chemical differences between the two CDs. Liu *et al.* exposed zebrafish embryos to CDs over the 1.5–96 h postfertilization period, and found no significant differences in mortality in the 50 – 200 mg L^{-1} range, however, a dose–response was observed at higher concentrations resulting in an LC_{50} of 257 mg L^{-1} .⁴² Yang *et al.* exposed mice to CDs *via* a single inhalation and found that a concentration of 5 mg kg^{-1} resulted in the survival of 80% of mice after 15 days, whereas 100% survival was measured in the control.⁴³ The single dose toxicity of CDs on mice *via* intravenous exposure was examined by Zheng *et al.*, finding that the LD_{50} in female mice was 392 mg kg^{-1} and for male mice was 358 mg kg^{-1} .⁴⁴ Ambrosone *et al.* exposed *Hydra vulgaris* to thioglycolic acid coated CdTeQDs for 72 h monitored daily.¹¹ They found that after 24 h of exposure the LC_{50} was 1.4 mg L^{-1} Cd equivalent, and that this dropped to 0.72 mg L^{-1} Cd equivalent after 72 h.¹¹ Another study found that exposing *Biomphalaria glabrata* embryos to 5 nM ($\sim 0.25 \text{ mg L}^{-1}$) CdTeQDs for 24 h resulted in 100% of embryos being deemed unviable.⁴⁵ Adult *Biomphalaria glabrata* had a higher tolerance, with 100% mortality observed 48 h after a 24 h exposure to 400 nM ($\sim 20 \text{ mg L}^{-1}$) CdTeQDs.⁴⁵ Our results, show similar trends to those found in the literature, which indicate that CdTeQDs exhibit considerably more toxicity than CDs.

3.3 Reproductive performance

Our developmental toxicity assay showed clear toxicity stemming from the exposure of *Drosophila melanogaster* to CdTeQDs with an EC_{50} of 46 mg kg^{-1} food. Conversely, no toxicity was observed from the NCDs or SCDs in the 10 – 100 mg kg^{-1} range

evaluated. However, there are many forms in which toxicity can manifest in an organism that do not necessarily lead to death. To ensure a comprehensive evaluation of carbon dot toxicity, we measured the impact of these nanoparticles on the reproductive performance of flies. Since no toxicity was observed in the NCDs and SCDs, further experiments were conducted at 100 mg kg^{-1} since this concentration was shown to not induce toxicity. However, this same concentration could not be used when evaluating CdTeQD toxicity, since we have already shown that it exhibits severe lethality and developmental delays (Fig. 1). Instead, we conducted further sublethal assessment of CdTeQDs at 5 mg kg^{-1} , a concentration approximately equal to the EC_1 or the concentration that would result in the failure of 1% of larvae to successfully develop into adult flies. No significant differences between treatments or experimental blocks were observed in the number of pupae or flies that emerged from the eggs laid over the span of ten days (Fig. 2). The time-series data (Fig. S11†) showed that reproductive performance typically increased or remained approximately constant during the 2–10 day period. These results indicate a lack of reproductive toxicity from these particles at a sublethal concentration.

Han *et al.* examined the effect of CDs on the reproduction of *Bursaphelenchus xylophilus*, and found that a 6000 mg L^{-1} concentration reduced the number of eggs laid.⁴⁶ A study examining the effects of thioglycolic acid coated CdTeQDs on the reproduction of *Hydra vulgaris* found that exposure to CdTeQD concentrations as low as 1 mg L^{-1} Cd for 14 days reduced their budding rate by 42% relative to the control.¹¹ Another study also examined the toxicity of CdTeQDs on the reproductive performance of *Drosophila melanogaster* and found a dose-dependent decline in fecundity, fertility, and hatchability in the 1 – $100 \mu\text{M}$ (approximately 100 – $10\,000 \text{ mg L}^{-1}$) range.⁴⁷ The toxicity of CdTeQDs in *Caenorhabditis elegans* was investigated by Qu *et al.*⁴⁸ They found no significant difference in the egg-laying rate at 5 – 25 mg L^{-1} relative to the control, but observed a dose-dependent decrease at 50 – 100 mg L^{-1} .⁴⁸ Similarly, our results are mostly consistent with the literature, showing that toxicity can vary between organisms and nanoparticles.

3.4 Fly mass assay

When given a fixed food source, the mass of a particular healthy organism is typically stable and predictable. The flies in each treatment were raised on identical food sources, with the only difference being the presence of NCDs (100 mg kg^{-1}), SCDs (100 mg kg^{-1}), or CdTeQDs (5 mg kg^{-1}). Considering that the highest of these concentrations (*i.e.*, 100 mg kg^{-1}) is equivalent to 0.01 wt% food, we can assume that food displacement is unlikely to be a contributing factor to any changes in mass observed. No significant differences between treatments were found in the mass of female flies, however the difference between experimental blocks was significant ($p = 0.024$) (Fig. 3a). It is worth noting that a large contribution to this difference in blocks was due to one particularly high mass measurement observed in block 2 (Fig. 3a). Significant differences between treatments ($p = 0.012$) and experimental block (p



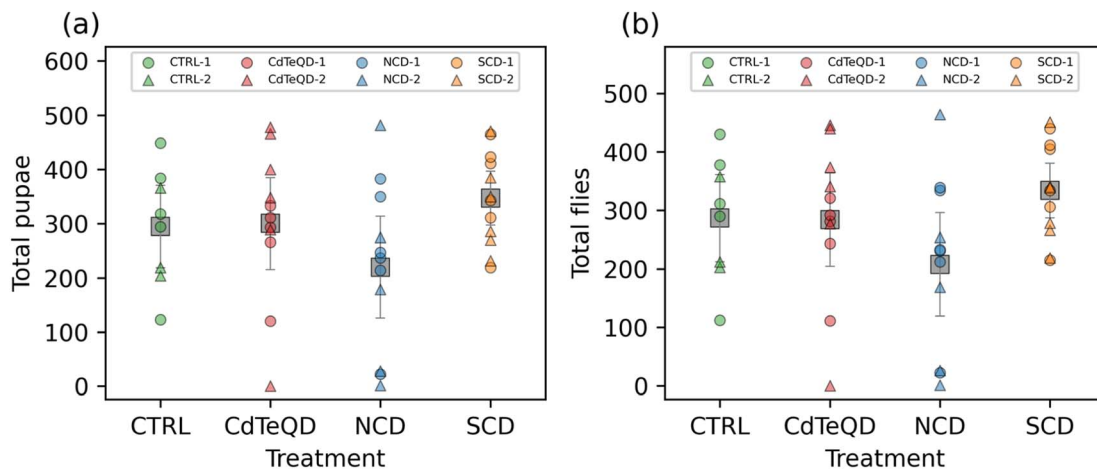


Fig. 2 Number of (a) pupae and (b) flies that emerged after allowing one female and one male fly that were raised on CTRL (0 mg kg^{-1}), NCD (100 mg kg^{-1}), SCD (100 mg kg^{-1}), or CdTeQD (5 mg kg^{-1}) treated food to mate for 10 days. Grey squares represent the mean of data points in that column and error bars represent $2 \times$ the standard error of the mean. Legend labels have the format $X-Y$ where X is the treatment and Y is the experimental block ID.

$= 0.037$) were observed in the mass of male flies (Fig. 3b). Due to the significant differences observed between blocks, we only consider significant differences between treatments if they occur within the same block. A post hoc analysis revealed that in block 2, the male flies raised on 100 mg kg^{-1} SCD had a significantly greater mass ($p < 0.05$) than those raised on 100 mg kg^{-1} NCD and the CTRL food. No significant differences were observed between treatments in block 1. The implication of these results, especially when considering the results in Fig. S10† showing a significant, but weak, correlation pointing towards larvae raised on SCDs having a slightly faster development time than the other treatments, suggest that SCDs might elicit a minor biological response in *Drosophila melanogaster* at 100 mg kg^{-1} food.

Zheng *et al.* exposed mice to a daily intravenous 100 mg kg^{-1} dose of CDs for 7 days and monitored their mass over 90 days

finding no notable difference in the overall mouse mass throughout the period evaluated.⁴⁴ In a study by Du *et al.*, CdTeQDs functionalized with thioglycolic acid and mercapto-acetohydrazine reduced the growth rate of mice relative to the control over the 7 days following 10 mg kg^{-1} intravenous injection of the CdTeQDs.⁴⁹ Interestingly, this reduction was no longer significantly different from the control when the CdTeQDs were further functionalized with polyethylene glycol.⁴⁹ Another study also examined the toxicity of CdTeQDs in mice and found that there were no significant differences in mass between the control and the $4.12\text{--}16.5 \text{ mg kg}^{-1}$ range measured.⁹ Similarly, our results coincided with these literature findings when considering the concentrations evaluated. While some significant differences were observed, they were not present in all experimental blocks.

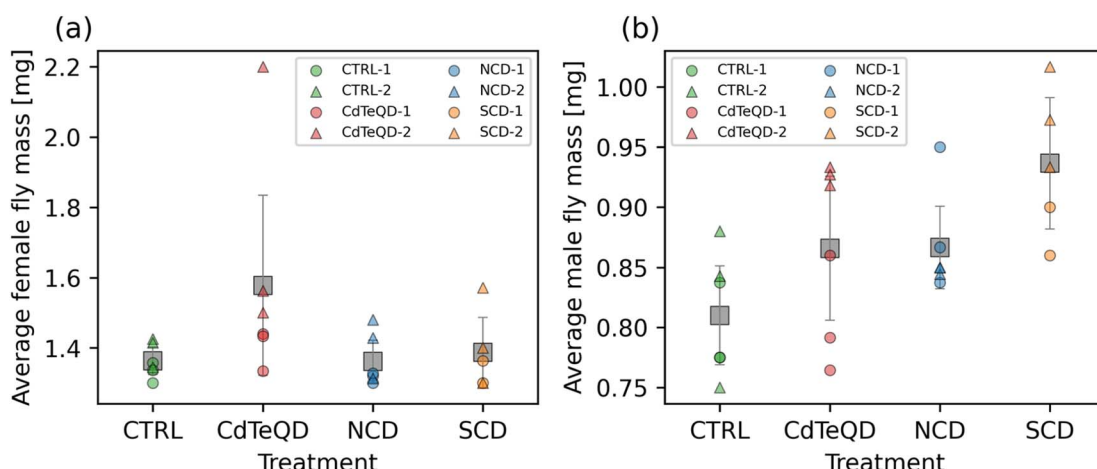


Fig. 3 Average mass of (a) female and (b) male flies that were raised on CTRL (0 mg kg^{-1}), NCD (100 mg kg^{-1}), SCD (100 mg kg^{-1}), or CdTeQD (5 mg kg^{-1}) treated food. Grey squares represent the mean of data points in that column and error bars represent $2 \times$ the standard error of the mean. Legend labels have the format $X-Y$ where X is the treatment and Y is the experimental block ID.

3.5 Larvae crawling and fly climbing assays

To fully understand the sublethal toxicity, it is essential to examine various developmental stages. In the reproductive performance assay, we measured the impact that parental exposure may have on their ability to produce offspring. We subsequently assessed the activity of the larvae that were raised under different conditions: CTRL (0 mg kg⁻¹), NCDs (100 mg kg⁻¹), SCDs (100 mg kg⁻¹), or CdTeQDs (5 mg kg⁻¹). No significant differences between treatments or experimental blocks were observed in the number of contractions per minute of the larvae (Fig. 4a). Similarly, when evaluating the climbing ability of the flies, no significant differences between treatments or experimental blocks were observed in the number of flies able to climb 10 cm within 10 s (Fig. 4b).

Liu *et al.* examined the effect of CDs on zebrafish larvae locomotion and found no significant difference in the distance travelled by larvae exposed to 50–150 mg L⁻¹ CDs, but a dose-response was observed whereby the travel distance declined in the 200–2000 mg L⁻¹ range.⁴² Similarly, Han *et al.* showed a decline in the number of thrashes per minute of *Bursaphelenchus xylophilus* in the 4000–6000 mg L⁻¹ CD range.⁴⁶ Paithankar *et al.* exposed *Drosophila melanogaster* to CdTeQDs in the concentration range of 0.2–100 μ M (approximately 20–10 000 mg L⁻¹) and saw no significant difference in the climbing ability of flies when compared to the control.⁴⁷ Although the literature sometimes reports that CDs and CdTeQDs can negatively impact the locomotion or climbing ability of organisms, these effects were typically observed at concentrations higher than those used in our study.

3.6 Locomotor activity

The larvae crawling assay is valuable for gauging the activity of *Drosophila melanogaster* during their development into adult flies. Once adults, the climbing assay is also a convenient tool for measuring the ability of flies to conduct a physically demanding task. One limitation to both these assays is the

relatively short time span over which data is recorded, typically on the order of a few seconds or minutes. Using an activity monitor, we were able to monitor the movement of adult male flies in one-minute intervals over three days. Averaging the daily activity over 72 h removes any variance that may come from the time of day that the measurement was taken at. It also provides an overall measure of activity since it also includes the night cycle of the flies. Significant differences between treatments ($p = 0.032$) and experimental blocks ($p = 0.024$) in the number of activity counts per day (*i.e.*, infrared beam breaks per day) were

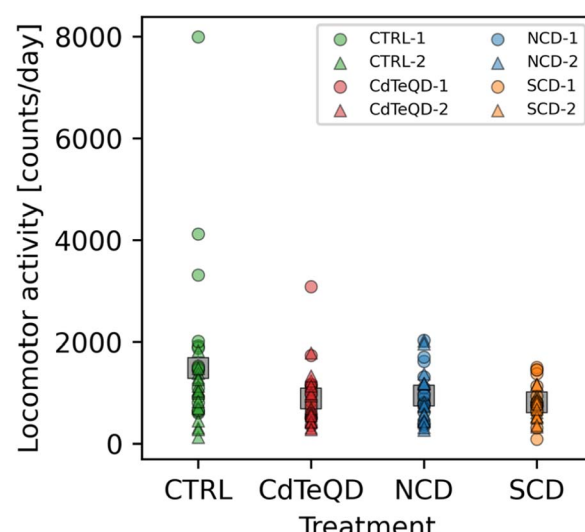


Fig. 5 Locomotor activity measured as average number of infrared beam breaks per day of male flies raised on CTRL (0 mg kg⁻¹), NCD (100 mg kg⁻¹), SCD (100 mg kg⁻¹), or CdTeQD (5 mg kg⁻¹) treated food. Grey squares represent the mean of data points in that column and error bars represent 2 \times the standard error of the mean. The standard errors are relatively small due to the large sample size and may be difficult to see in the figure. Legend labels have the format X–Y where X is the treatment and Y is the experimental block ID.

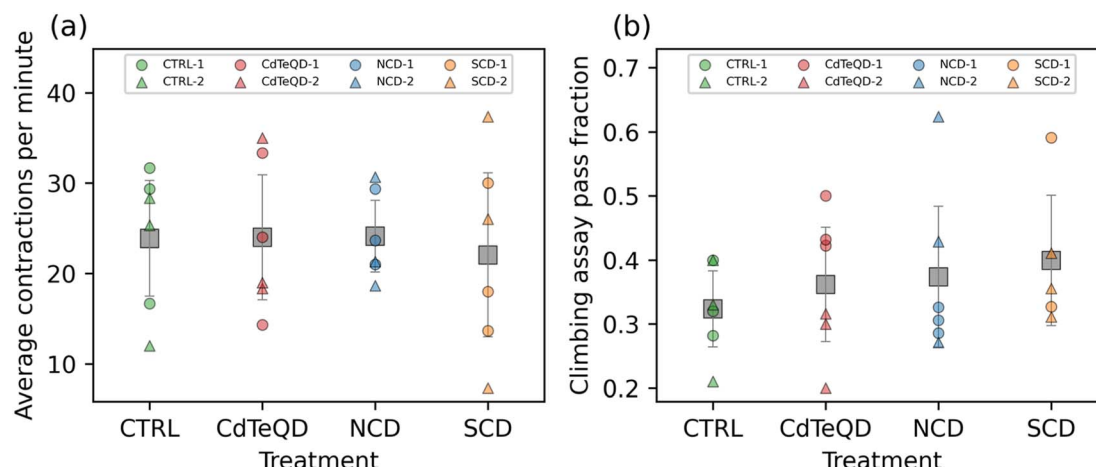


Fig. 4 (a) Average number of larval contractions per minute and (b) fraction of flies able to climb 10 cm within 10 s. Larvae and flies were raised on CTRL (0 mg kg⁻¹), NCD (100 mg kg⁻¹), SCD (100 mg kg⁻¹), or CdTeQD (5 mg kg⁻¹) treated food. Grey squares represent the mean of data points in that column and error bars represent 2 \times the standard error of the mean. Legend labels have the format X–Y where X is the treatment and Y is the experimental block ID.



observed (Fig. 5). A post hoc analysis revealed that these significant differences stemmed from the CTRL activity in block 1 being more than double the SCD and CdTeQD activities in block 2. However, since there were significant differences observed between blocks, a comparison of treated flies from block 2 with the CTRL in block 1, is not very meaningful even if the difference is significant. Moreover, Fig. 5 clearly shows that three replicates from the CTRL in block 1 had unusually high activity which may have skewed the mean upward.

3.7 Nanoparticle uptake analysis

Nanoparticle-exposed flies were imaged using LSFM (Fig. 6, S12–S15†). Due to the difference in optical signatures of the particles, different filters and excitation wavelengths were utilized. An excitation wavelength of 405 nm with a bandpass filter at 420–470 nm was used to illustrate the autofluorescence of the fruit fly. The fluorescence of the NCDs was not evident since its emission spectrum (Fig. S6†) was similar to that of the fly's autofluorescence. Conversely, SCDs were visualized in red by using a 640 nm long pass filter under 405 nm excitation. Signals stemming from the CdTeQDs were obtained using an excitation wavelength of 561 nm and a long pass filter at 640 nm. In the case of SCDs and CdTeQDs, it was apparent that the particles were localized inside and on the surface of the organism (Fig. 6), however the degree of this internalization varied across replicates (Fig. S13 and S15†).

3.8 Nano-CT imaging

Nano-CT imaging of the fruit flies was performed to examine internal anatomical differences (Fig. S16–S19†). At the midgut in

the thorax, all samples seemed normal except in CdTeQD1 (first of two replicates) (Fig. S17†) where the anterior midgut was expanded near the thorax-abdomen boundary. The first loop of the distal anterior midgut within the abdomen was comparable between the controls and treatments. However, the middle midgut (cooper cell region) was extended and formed an extra loop within the anterior and posterior midgut coils in all imaged treatment samples. This was in contrast to the single middle midgut loop in the controls. A similar result was reported by Matthews *et al.*²⁴ The length of the posterior midgut, as it extends from the middle, bulged anterolaterally to the cuticle in nearly all treatment samples. It contacted the cuticle in the controls but distended the surface of the anterolateral abdomen in NCD1, SCD1, SCD3, and CdTeQD2 with the latter being the most extreme (Fig. S17–S19†). This could imply that 5 mg kg^{−1} CdTeQD was still more toxic than 100 mg kg^{−1} CD in inducing gut distension. However, this would also imply that 100 mg kg^{−1} CD could potentially still be too high a concentration if this sublethal toxic effect was observed. Therefore, further investigation covering a wider range of concentrations with a larger sample size is needed before an upper concentration limit on safe CD exposure can be established. Gut tube virtual histologies are comparable across all imaged control and treatment samples. Only the proximal posterior midgut was distinctly thinner and appeared ruptured in CdTeQD1 (Fig. S17†). The middle midguts of SCD1 and SCD3 were thinner walled and also apparently ruptured (Fig. S19†). Although the cause of these gut tube expansions is unknown, we speculate that they may be filled with indigestible nanoparticles. Traditional histological analyses with serial sections would be required to advance research into the physiological effects of the nanoparticle types on the gut tube. Some differences with oenocytes were observed. Oenocytes are abdominal cells that have recently been postulated to perform vertebrate liver-like functions.⁵⁰ They are visible in the CT data and generally fill much of the abdomen not occupied by the gut tube. Of the three controls imaged, two showed normal anatomies whereas one (CTRL1) had a markedly reduced number of oenocytes with poor X-ray contrast within a much-reduced abdomen, the causes of which are unknown. Oenocytes in the NCD treatments were reduced in number. Those in the SCD treatments appeared relatively normal in number and size with the exception of their asymmetrical distribution likely due to the extreme distended posterior midguts in these specimens. The CdTeQD treatments presented a unique phenotype with either many more smaller oenocytes packed into the abdomen (CdTeQD1) or fewer oenocytes that have poor X-ray contrast (CdTeQD2). This specimen was somewhat comparable to CTRL1 and may simply illustrate variation in oenocytes among individuals. However, the number and distribution of oenocytes throughout the treatments may lead to further biological assays on non-lethal effects.

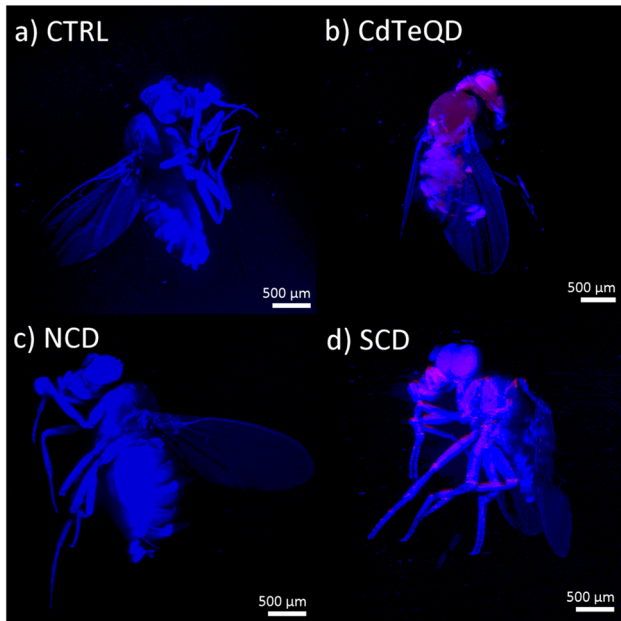


Fig. 6 LSFM images of female flies from day 11 raised on (a) CTRL (0 mg kg^{−1}), (b) CdTeQD (5 mg kg^{−1}), (c) NCD (100 mg kg^{−1}), or (d) SCD (100 mg kg^{−1}) treated food. Red fluorescence originates from SCDs and CdTeQDs. Blue fluorescence was from the fly's autofluorescence. NCDs also emit blue light and were therefore not easily discernible.

4 Conclusions

While there was no developmental toxicity from NCDs or SCDs observed, a dose-dependant toxicity was observed from the CdTeQDs with a larva-to-fly EC₅₀ of 46 ± 4.7 mg kg^{−1} food (mean



± standard error). We also saw no correlation between NCD concentration in food and emergence time but saw a weak negative correlation for SCDs and a strong positive correlation for CdTeQDs indicating that CdTeQDs can delay the development of larvae into pupae and flies. Using sublethal concentrations of 100 mg kg⁻¹ for NCDs and SCDs and 5 mg kg⁻¹ for CdTeQDs, further assays concluded that the SCD-exposed male flies had a significantly greater mass than those raised on CTRL and NCD food in experimental block 2, but not in block 1. Moreover, while significant differences were observed between treatments in the locomotor activity of flies, these differences occurred between blocks, and therefore were not indicative of a potential response. No significant difference between any of the treatments when evaluating reproductive performance, larval crawling, and fly climbing ability were observed. Deformations to the gut tube were observed in all imaged treatment samples. These included extended middle midguts that expressed a second loop within the abdomen, in contrast to the single loop in the shorter comparable regions in the controls. Although internal physiological responses to CDs are more difficult to assay, this study introduces several gut tube effects that may not be reflected in traditional external assays, such as locomotion, reproduction, and pupation rates. Such results suggest that longer term and more challenging, non-laboratory conditions may be used to develop more sensitive experimental assays.

This work shows that two chemically diverse carbon dots containing a variety of elements and functional groups were considerably less toxic than CdTeQDs in the model organism *Drosophila melanogaster*. Other than signs of gut distension which were observed to varying degrees in nanoparticle-treated flies, the fact that CdTeQDs showed no sublethal toxicity at 5 mg kg⁻¹ but had an EC₅₀ of just 46 mg kg⁻¹, suggests that there is a narrow range of concentrations whereby CdTeQD toxicity rapidly increases. SCDs might induce a minor biological response in *Drosophila melanogaster* at a concentration of 100 mg kg⁻¹. Further research may be warranted on other organisms, and perhaps at a higher concentration, to determine the nature of this potential response. The direct comparison of CDs and CdTeQDs allows us to gain insight into the relative toxicity of these two types of nanoparticles.

Conflicts of interest

There are no conflicts to declare.

Acknowledgements

The authors acknowledge financial support from the Natural Sciences and Engineering Research Council of Canada (NSERC) for the Discovery, Strategic, and PURE CREATE programs, the Canada Research Chairs Program, the Killam Research Fellowship, the Canada Foundation for Innovation, and the FRQNT. RN is also grateful for financial support from Concordia University's Research Chair Program. SC acknowledges NSERC for a PGS D scholarship, EcotoQ (FRQNT), and McGill University for a MEDA fellowship and the support of the EUL fund in the Department of Chemical Engineering. J.-R. M.

acknowledges NSERC for a Postdoctoral Fellowship. This research was performed using infrastructure from the Integrated Quantitative Biology Initiative, funded by the Quebec government, McGill University, and the Canadian Foundation of Innovation project 33122. The authors thank Sara Matthews and Eva Roubeau Dumont for helpful discussions.

References

- Y. Pu, F. Cai, D. Wang, J.-X. Wang and J.-F. Chen, Colloidal Synthesis of Semiconductor Quantum Dots toward Large-Scale Production: A Review, *Ind. Eng. Chem. Res.*, 2018, **57**, 1790–1802.
- Y. Zhang, Y. Li and X.-P. Yan, Aqueous Layer-by-Layer Epitaxy of Type-II CdTe/CdSe Quantum Dots with Near-Infrared Fluorescence for Bioimaging Applications, *Small*, 2009, **5**, 185–189.
- Y. Choi, M. Seol, W. Kim and K. Yong, Chemical Bath Deposition of Stoichiometric CdSe Quantum Dots for Efficient Quantum-Dot-Sensitized Solar Cell Application, *J. Phys. Chem. C*, 2014, **118**, 5664–5670.
- S. Bera, S. B. Singh and S. K. Ray, Green route synthesis of high quality CdSe quantum dots for applications in light emitting devices, *J. Solid State Chem.*, 2012, **189**, 75–79.
- K.-Y. Yi, Application of CdSe quantum dots for the direct detection of TNT, *Forensic Sci. Int.*, 2016, **259**, 101–105.
- C. B. Murray, D. J. Norris and M. G. Bawendi, Synthesis and characterization of nearly monodisperse CdE (E = sulfur, selenium, tellurium) semiconductor nanocrystallites, *J. Am. Chem. Soc.*, 1993, **115**, 8706–8715.
- W. Liu, S. Zhang, L. Wang, C. Qu, C. Zhang, L. Hong, L. Yuan, Z. Huang, Z. Wang, S. Liu and G. Jiang, CdSe Quantum Dot (QD)-Induced Morphological and Functional Impairments to Liver in Mice, *PLoS One*, 2011, **6**, e24406.
- M. Green and E. Howman, Semiconductor quantum dots and free radical induced DNA nicking, *Chem. Commun.*, 2005, 121–123, DOI: [10.1039/b413175d](https://doi.org/10.1039/b413175d).
- T. Zhang, Y. Hu, M. Tang, L. Kong, J. Ying, T. Wu, Y. Xue and Y. Pu, Liver Toxicity of Cadmium Telluride Quantum Dots (CdTe QDs) Due to Oxidative Stress *in Vitro* and *in Vivo*, *Int. J. Mol. Sci.*, 2015, **16**(10), 23279–23299.
- W. Zhang, K. Lin, Y. Miao, Q. Dong, C. Huang, H. Wang, M. Guo and X. Cui, Toxicity assessment of zebrafish following exposure to CdTe QDs, *J. Hazard. Mater.*, 2012, **213–214**, 413–420.
- A. Ambrosone, L. Mattera, V. Marchesano, A. Quarta, A. S. Susha, A. Tino, A. L. Rogach and C. Tortiglione, Mechanisms underlying toxicity induced by CdTe quantum dots determined in an invertebrate model organism, *Biomaterials*, 2012, **33**, 1991–2000.
- T. Liu, R. Xing, Y.-F. Zhou, J. Zhang, Y.-Y. Su, K.-Q. Zhang, Y. He, Y.-H. Sima and S.-Q. Xu, Hematopoiesis toxicity induced by CdTe quantum dots determined in an invertebrate model organism, *Biomaterials*, 2014, **35**, 2942–2951.
- S. Chahal, J.-R. Macairan, N. Yousefi, N. Tufenki and R. Naccache, Green synthesis of carbon dots and their applications, *RSC Adv.*, 2021, **11**, 25354–25363.



14 S. Qu, X. Wang, Q. Lu, X. Liu and L. Wang, A Biocompatible Fluorescent Ink Based on Water-Soluble Luminescent Carbon Nanodots, *Angew. Chem., Int. Ed.*, 2012, **51**, 12215–12218.

15 C. Ong, L.-Y. L. Yung, Y. Cai, B.-H. Bay and G.-H. Baeg, *Drosophila melanogaster* as a model organism to study nanotoxicity, *Nanotoxicology*, 2015, **9**, 396–403.

16 L. T. Reiter, L. Potocki, S. Chien, M. Gribskov and E. Bier, A systematic analysis of human disease-associated gene sequences in *Drosophila melanogaster*, *Genome Res.*, 2001, **11**, 1114–1125.

17 U. B. Pandey and C. D. Nichols, Human Disease Models in *Drosophila melanogaster* and the Role of the Fly in Therapeutic Drug Discovery, *Pharmacol. Rev.*, 2011, **63**, 411.

18 M. Alaraby, E. Demir, A. Hernández and R. Marcos, Assessing potential harmful effects of CdSe quantum dots by using *Drosophila melanogaster* as *in vivo* model, *Sci. Total Environ.*, 2015, **530–531**, 66–75.

19 A. Xiao, C. Wang, J. Chen, R. Guo, Z. Yan and J. Chen, Carbon and Metal Quantum Dots toxicity on the microalgae *Chlorella pyrenoidosa*, *Ecotoxicol. Environ. Saf.*, 2016, **133**, 211–217.

20 G. Magdy, S. Ebrahim, F. Belal, R. A. El-Domany and A. M. Abdel-Megied, Sulfur and nitrogen co-doped carbon quantum dots as fluorescent probes for the determination of some pharmaceutically-important nitro compounds, *Sci. Rep.*, 2023, **13**, 5502.

21 S. Chahal, N. Yousefi and N. Tufenkji, Green Synthesis of High Quantum Yield Carbon Dots from Phenylalanine and Citric Acid: Role of Stoichiometry and Nitrogen Doping, *ACS Sustain. Chem. Eng.*, 2020, **8**, 5566–5575.

22 J.-R. Macairan, D. B. Jaunay, A. Piecky and R. Naccache, Intracellular ratiometric temperature sensing using fluorescent carbon dots, *Nanoscale Adv.*, 2019, **1**, 105–113.

23 S. A. Pappus, B. Ekka, S. Sahu, D. Sabat, P. Dash and M. Mishra, A toxicity assessment of hydroxyapatite nanoparticles on development and behaviour of *Drosophila melanogaster*, *J. Nanopart. Res.*, 2017, **19**, 136.

24 S. Matthews, E. G. Xu, E. Roubeau Dumont, V. Meola, O. Pilkuda, R. S. Cheong, M. Guo, R. Tahara, H. C. E. Larsson and N. Tufenkji, Polystyrene micro- and nanoplastics affect locomotion and daily activity of *Drosophila melanogaster*, *Environ. Sci.: Nano*, 2021, **8**, 110–121.

25 N. R. Bartholomew, J. M. Burdett, J. M. VandenBrooks, M. C. Quinlan and G. B. Call, Impaired climbing and flight behaviour in *Drosophila melanogaster* following carbon dioxide anaesthesia, *Sci. Rep.*, 2015, **5**, 15298.

26 P. P. Pompa, G. Vecchio, A. Galeone, V. Brunetti, S. Sabella, G. Maiorano, A. Falqui, G. Bertoni and R. Cingolani, *In Vivo* toxicity assessment of gold nanoparticles in *Drosophila melanogaster*, *Nano Res.*, 2011, **4**, 405–413.

27 M. B. Feany and W. W. Bender, A *Drosophila* model of Parkinson's disease, *Nature*, 2000, **404**, 394–398.

28 T. Niccoli, M. Cabecinha, A. Tillmann, F. Kerr, C. T. Wong, D. Cardenes, A. J. Vincent, L. Bettledi, L. Li, S. Grönke, J. Dols and L. Partridge, Increased Glucose Transport into Neurons Rescues A β Toxicity in *Drosophila*, *Curr. Biol.*, 2016, **26**, 2291–2300.

29 J.-R. Macairan, B. Nguyen, F. Li and N. Tufenkji, Tissue Clearing To Localize Microplastics *via* Three-Dimensional Imaging of Whole Organisms, *Environ. Sci. Technol.*, 2023, **57**, 8476–8483.

30 H. Hama, H. Hioki, K. Namiki, T. Hoshida, H. Kurokawa, F. Ishidate, T. Kaneko, T. Akagi, T. Saito, T. Saido and A. Miyawaki, ScaleS: an optical clearing palette for biological imaging, *Nat. Neurosci.*, 2015, **18**, 1518–1529.

31 *Software, Dragonfly*, ORS, 2020.

32 *Software, Blender*, Blender Foundation, 2018.

33 C. R. Harris, K. J. Millman, S. J. van der Walt, R. Gommers, P. Virtanen, D. Cournapeau, E. Wieser, J. Taylor, S. Berg, N. J. Smith, R. Kern, M. Picus, S. Hoyer, M. H. van Kerkwijk, M. Brett, A. Haldane, J. F. del Río, M. Wiebe, P. Peterson, P. Gérard-Marchant, K. Sheppard, T. Reddy, W. Weckesser, H. Abbasi, C. Gohlke and T. E. Oliphant, Array programming with NumPy, *Nature*, 2020, **585**, 357–362.

34 W. McKinney, *Proceedings of the 9th Python in Science Conference*, 2010.

35 *Software, Pandas-Dev/pandas: Pandas*, The pandas development team, 2022, DOI: [10.5281/zenodo.6408044](https://doi.org/10.5281/zenodo.6408044).

36 P. Virtanen, R. Gommers, T. E. Oliphant, M. Haberland, T. Reddy, D. Cournapeau, E. Burovski, P. Peterson, W. Weckesser, J. Bright, S. J. van der Walt, M. Brett, J. Wilson, K. J. Millman, N. Mayorov, A. R. J. Nelson, E. Jones, R. Kern, E. Larson, C. J. Carey, İ. Polat, Y. Feng, E. W. Moore, J. VanderPlas, D. Laxalde, J. Perktold, R. Cimrman, I. Henriksen, E. A. Quintero, C. R. Harris, A. M. Archibald, A. H. Ribeiro, F. Pedregosa, P. van Mulbregt, A. Vijaykumar, A. P. Bardelli, A. Rothberg, A. Hilboll, A. Kloekner, A. Scopatz, A. Lee, A. Rokem, C. N. Woods, C. Fulton, C. Masson, C. Häggström, C. Fitzgerald, D. A. Nicholson, D. R. Hagen, D. V. Pasechnik, E. Olivetti, E. Martin, E. Wieser, F. Silva, F. Lenders, F. Wilhelm, G. Young, G. A. Price, G.-L. Ingold, G. E. Allen, G. R. Lee, H. Audren, I. Probst, J. P. Dietrich, J. Silterra, J. T. Webber, J. Slavić, J. Nothman, J. Buchner, J. Kulick, J. L. Schönberger, J. V. de Miranda Cardoso, J. Reimer, J. Harrington, J. L. C. Rodríguez, J. Nunez-Iglesias, J. Kuczynski, K. Tritz, M. Thoma, M. Newville, M. Kümmerer, M. Bolingbroke, M. Tartre, M. Pak, N. J. Smith, N. Nowaczyk, N. Shebanov, O. Pavlyk, P. A. Brodtkorb, P. Lee, R. T. McGibbon, R. Feldbauer, S. Lewis, S. Tygier, S. Sievert, S. Vigna, S. Peterson, S. More, T. Pudlik, T. Oshima, T. J. Pingel, T. P. Robitaille, T. Spura, T. R. Jones, T. Cera, T. Leslie, T. Zito, T. Krauss, U. Upadhyay, Y. O. Halchenko, Y. Vázquez-Baeza and C. SciPy, SciPy 1.0: fundamental algorithms for scientific computing in Python, *Nat. Methods*, 2020, **17**, 261–272.

37 S. Seabold and J. Perktold, *9th Python in Science Conference*, 2010.

38 J. D. Hunter, Matplotlib: A 2D Graphics Environment, *Comput. Sci. Eng.*, 2007, **9**, 90–95.



39 J. Manioudakis, F. Victoria, C. A. Thompson, L. Brown, M. Movsum, R. Lucifer and R. Naccache, Effects of nitrogen-doping on the photophysical properties of carbon dots, *J. Mater. Chem. C*, 2019, **7**, 853–862.

40 J.-R. Macairan, T. V. de Medeiros, M. Gazzetto, F. Yarur Villanueva, A. Cannizzo and R. Naccache, Elucidating the mechanism of dual-fluorescence in carbon dots, *J. Colloid Interface Sci.*, 2022, **606**, 67–76.

41 I. Chousidis, C. D. Stalikas and I. D. Leonardos, Induced toxicity in early-life stage zebrafish (*Danio rerio*) and its behavioral analysis after exposure to non-doped, nitrogen-doped and nitrogen, sulfur-co doped carbon quantum dots, *Environ. Toxicol. Pharmacol.*, 2020, **79**, 103426.

42 W. Liu, G. Huang, X. Su, S. Li, Q. Wang, Y. Zhao, Y. Liu, J. Luo, Y. Li, C. Li, D. Yuan, H. Hong, X. Chen and T. Chen, Zebrafish: A Promising Model for Evaluating the Toxicity of Carbon Dot-Based Nanomaterials, *ACS Appl. Mater. Interfaces*, 2020, **12**, 49012–49020.

43 Y. Yang, X. Ren, Z. Sun, C. Fu, T. Liu, X. Meng and Z. Wang, Toxicity and bio-distribution of carbon dots after single inhalation exposure *in vivo*, *Chin. Chem. Lett.*, 2018, **29**, 895–898.

44 X. Zheng, D. Shao, J. Li, Y. Song, Y. Chen, Y. Pan, S. Zhu, B. Yang and L. Chen, Single and repeated dose toxicity of citric acid-based carbon dots and a derivative in mice, *RSC Adv.*, 2015, **5**, 91398–91406.

45 M. de Vasconcelos Lima, M. I. de Andrade Pereira, P. E. Cabral Filho, W. Nascimento de Siqueira, H. A. Milca Fagundes Silva, E. J. de França, B. Saegesser Santos, A. M. Mendonça de Albuquerque Melo and A. Fontes, Studies on Toxicity of Suspensions of CdTe Quantum Dots to *Biomphalaria glabrata* Mollusks, *Environ. Toxicol. Chem.*, 2019, **38**, 2128–2136.

46 Y. Han, Y. Han, G. Du, T. Zhang, Q. Guo, H. Yang, R. Li and Y. Xu, Physiological effect of colloidal carbon quantum dots on *Bursaphelenchus xylophilus*, *RSC Adv.*, 2021, **11**, 6212–6220.

47 J. G. Paithankar, S. Kushalan, N. S. S. Hegde, S. Kini and A. Sharma, Systematic toxicity assessment of CdTe quantum dots in *Drosophila melanogaster*, *Chemosphere*, 2022, **295**, 133836.

48 M. Qu, Y. Qiu, R. Lv, Y. Yue, R. Liu, F. Yang, D. Wang and Y. Li, Exposure to MPA-capped CdTe quantum dots causes reproductive toxicity effects by affecting oogenesis in nematode *Caenorhabditis elegans*, *Ecotoxicol. Environ. Saf.*, 2019, **173**, 54–62.

49 Y. Du, Y. Zhong, J. Dong, C. Qian, S. Sun, L. Gao and D. Yang, The effect of PEG functionalization on the *in vivo* behavior and toxicity of CdTe quantum dots, *RSC Adv.*, 2019, **9**, 12218–12225.

50 K. Huang, Y. Liu and N. Perrimon, Roles of Insect Oenocytes in Physiology and Their Relevance to Human Metabolic Diseases, *Front. Insect Sci.*, 2022, **2**, 85947.

